ELSEVIER

Journal of Hydrology 253 (2001) 14–26

Journal of Hydrology

www.elsevier.com/locate/jhydrol

Hydrogeochemistry of groundwaters from carbonate formations with basal gypsiferous layers: an example from the Mt Catria–Mt Nerone ridge (Northern Appennines, Italy)

Bruno Capaccioni[a,*], Mariano Didero[b], Carmela Paletta[b], Piero Salvadori[c]

[a]*Institute of Volcanology and Geochemistry, Univ. of Urbino, Urbino (PU), Italy*
[b]*Institute of Applied Geology, Univ. of Urbino, Urbino (PU), Italy*
[c]*Agenzia Regionale Protezione Ambientale Marche, Italy*

Received 7 July 2000; revised 17 April 2001

Abstract

The Mt Catria–Mt Nerone Mesozoic calcareous ridge contains a defined, almost isolated, hydrogeological system. This system is composed of three main superimposed aquifers, separated by marly and marly-clayey aquicludes, which developed in the calcareous and marly-calcareous formations of the Umbria–Marche series. The lower water circulation occurs in the 'Massiccio' formation, where Ca(Mg)–HCO_3 waters mix with underlying gypsum-saturated waters due to the presence of Triassic evaporites, giving rise to Ca(Mg)–HCO_3–SO_4 up to Ca(Mg)–SO_4 water types. The mixing ratio between the two end members or the degree of gypsum dissolution depends on the depth of water circulation and depth of the top of the Triassic evaporites. Recharge areas for these water types are located at the highest elevations on the ridge, while discharge areas occur at springs along the slopes of the main reliefs as well as in two deeply eroded valleys. Waters recharged in the Mt Nerone area (north-western side of the ridge) appear to be affected by gypsum and dolomite dissolution caused by a direct interaction at depth with the Triassic evaporites, followed by calcite precipitation in a closed P_{CO_2} system (dedolomitization). Conversely, waters recharged in the Mt Catria area (south-eastern side of the ridge) seem to be affected by gypsum-dissolution and calcite-precipitation in an open P_{CO_2} system, which produces fracture sealing of the upper parts (120 m) of the 'Massiccio' formation, and a confinement of the deep waters. The consequent pressurization causes additional gypsum dissolution without calcite precipitation in a closed P_{CO_2} system. Previous hypotheses of hydraulic continuity of the basal aquifer throughout the calcareous ridge are reconsidered here and a new interpretation based on hydrochemical data is provided.

Keywords: Groundwaters; Evaporites; Hydrogeochemistry; Appennines

1. Introduction

The contemporary occurrence of Mesozoic limestones and dolostones associated with Triassic gypsiferous layers of evaporitic origin, gives rise to Ca-sulphate-rich waters able to induce dissolution–precipitation processes in the dolomite–calcite mineral assemblage. Hanshaw and Back (1979) discussed geochemical processes in carbonate aquifer systems and their hydrogeological implications. Plummer et al. (1990) recognized that dedolomitization induced by gypsum dissolution is the main

* Corresponding author. Tel.: +39-722-304257; fax: +39-722-304245.
E-mail address: b.capaccioni@geo.uniurb.it (B. Capaccioni).

0022-1694/01/$ - see front matter
PII: S0022-1694(01)00480-2

controlling factor for the evolution of water chemistry in the Madison aquifer (Montana, USA). Analogous conditions exist in the Apennines in the Marches region (Central Italy) where a massive limestone unit ('Massiccio' formation, Sinemuriano–Pliensbachiano) lies over a sequence of Upper Triassic evaporites ('Anidriti di Burano' formation; Martinis and Pieri, 1964; Passeri, 1975). The 'Massiccio' formation is the main lithotype of the Mt Catria–Mt Nerone carbonatic ridge. This ridge is one of the most important water reservoirs in the northern sector of the Marches region.

Overflow springs with significant discharge rates (100–200 l/s) emerge from the limestone formations at different elevations and drillings in the deeply eroded Burano Valley have revealed the existence of a highly productive pressurised aquifer at depth. Wells display discharge rates as high as 300–400 l/s. The impervious layer which likely confines the lowermost aquifer in the area, consists of a zone of calcite fracture sealing (about 120 m thick) affecting the shallow portion of the 'Massiccio' formation (Bison et al., 1995). Pressurization of the lowermost aquifer seems to be limited to the topographic and structural depression of the Burano valley, and is almost completely absent in the other outcrop areas of the 'Massiccio' formation. Fracture sealing seems to constitute a fundamental phenomenon in controlling fluid motion at depth. Using hydrogeological and hydrochemical data on the springs and water wells in the area under study, inferences are made regarding the hydrogeological structure of the Mt Catria–Mt Nerone calcareous ridge and the possible genetic mechanism of the observed calcite sealing inside the 'Massiccio' formation is discussed.

2. Geology and hydrogeology of the area under study

The area under study is located in the easternmost sector of the Northern Apennines, where the main watershed dividing the Umbria and Marches regions occurs (Fig. 1). According to Tavarnelli (1997), Barchi et al. (1998) and Buiter et al. (1998), the Umbria–Marches Apennines can be considered a typical thin-skinned thrust belt in which a hierarchy of multiple, superimposed detachments occurred over a main, basal detachment at the level of Triassic evaporites.

According to Alvarez (1989a,b) and Barchi et al. (1998) the stratigraphy in the area consists of: (i) an Upper Palaeozoic phyllitic basement, known only by drillings (Bison et al., 1995); (ii) an Upper Triassic evaporitic sequence followed by a Lower Liassic carbonatic platform sequence ('Massiccio' limestone) and by Jurassic–Paleogene pelagic cherty, marly and calcareous formations; and (iii) a syn-tectonic turbidite sequence (Lower Miocene–Pliocene). The area under study (Fig. 1), about 120 km^2, includes the following main reliefs: Mt Nerone (1525 m a.s.l.), Mt Montagnola (972 m a.s.l.), Mt Petrano (1106 m a.s.l.), Mt Acuto (1668 m a.s.l.) and Mt Catria (1658 m a.s.l.). The minimum elevations in the area are found in the Burano and Bosso valleys (two deeply dissected transversal-to-the-ridge valleys, ranging between 296–400 and 315–385 m a.s.l., respectively) and along the Vitoschio and Candigliano rivers (360–750 m a.s.l.) on the north-western boundary of the ridge. The 'Massiccio' formation constitutes the main portion of the Mesozoic carbonates; it crops out in both the Bosso and the Burano valleys, and along the northern and southern boundaries of the ridge at its main topographic elevations (Fig. 1). In the intermediate sectors it is covered by younger deposits.

The ridge consists of an antiformal structure with an axis elongated NW–SE. It is limited northwestwards by a continuous front-limb thrust fault, while northwards and southwards the thrust fault is displaced by Apennine and Antiapennine fault systems. Marly-clayey units of the younger synorogenic formations of the upper Umbrian Marches series are found northeastward and southwestward of the ridge.

This stratigraphic and structural setting forces a parallel-to-the-ridge circulation of groundwaters, and the ridge itself has been considered as an isolated hydrogeological system (Bison et al., 1995). According to Centamore et al. (1976), the carbonatic ridge hosts three superimposed aquifers, which are pervious due to secondary permeability (Fig. 2). Starting from the top they are located in the following formations:

Aqf 1: in limestones and marly-limestones of the 'Scaglia Rossa' and 'Scaglia Bianca' formations;
Aqf 2: in limestones and dolomitic limestones of

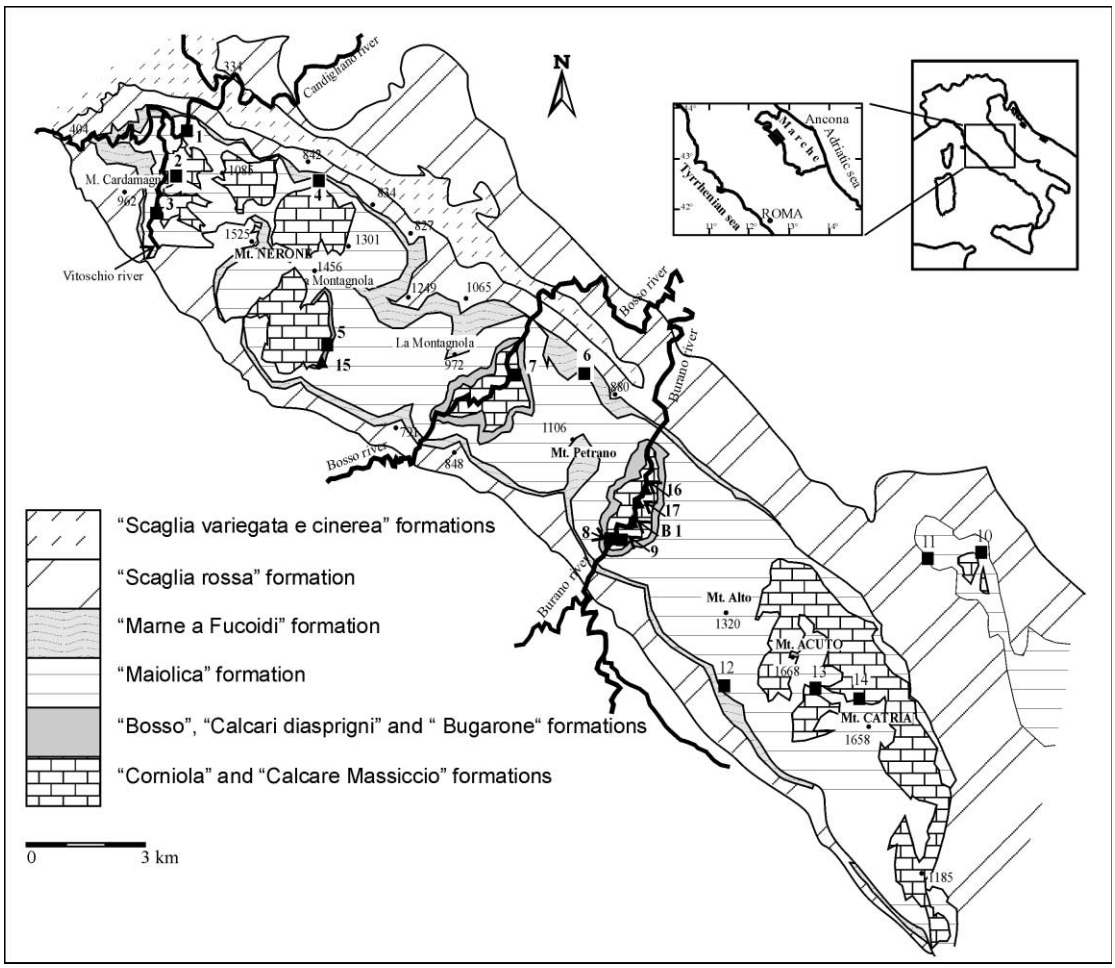

Fig. 1. Simplified geological map of the investigated area with locations of the sample points. Closed squares, springs; closed triangles, wells.

the 'Maiolica' formation;
Aqf 3: in stratified limestones of the 'Corniola' and massive limestones of the 'Massiccio' formations.

The aquicludes consist of:

Aqc 1: in marlstones and clayey-marlstones of the 'Marne a fucoidi' formation;
Aqc 2: in marly-limestones of the 'Rosso Ammonitico', nodular limestones of 'Bugarone' and 'Calcari selciferi diasprigni' formations.

Hydraulic connections can occur, locally, between Aqf 3 and Aqf 2 due to the lack of the interposed Aqc 2, whose thickness varies considerably (0–50 m) (Fig. 2). The Aqf 3 is located in the 'Massiccio' formation and, locally, in the most calcareous terms of the 'Corniola' formation. The increasing thickness of marly terms in the upper portion of the 'Corniola' formation (Jacobacci et al., 1974) strongly affects its secondary permeability, decreasing the total thickness of Aqf 3 and, consequently, increasing the importance of Aqc 2. Basal Aqf 3 directly overlies the Triassic evaporites which, according to Martinis and Pieri (1964), are composed of limestones and marls (with 'Raethavicula Contorta' auct.) dolomitic limestones, anhydrites and gypsum. Triassic evaporites do not crop out in the area and they were only encountered during drilling for oil exploration (Burano I well; Martinis and Pieri, 1964; Bison et al., 1995). The

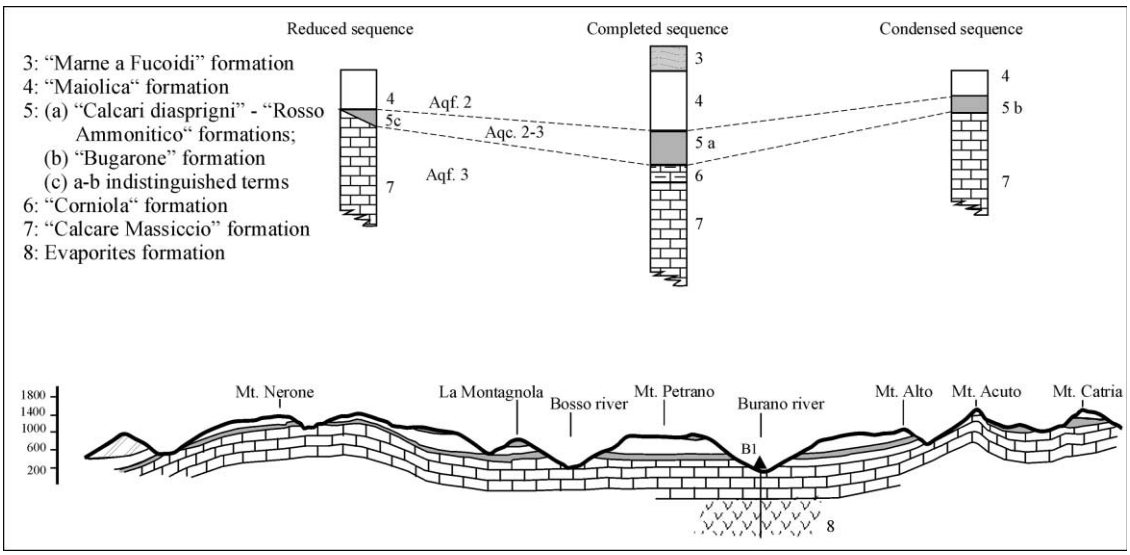

Fig. 2. Schematic NW–SE cross section and basic stratigraphy of the area under study.

recharge for the described hydrogeological units are mainly from the outcrop areas of Aqf 2 and Aqf 3, which mostly occur at the high topographic areas of Mt Nerone, Mt Acuto and Mt Catria.

According to Fig. 2, the NW–SE folded structure roughly follows the surface morphology. This implies that the lowest elevations of the top of the Triassic evaporites (−305 m measured during drilling of the Burano well) coincide with the morphological lows of the Burano and Bosso valleys. According to previous studies (Bison et al., 1995), basal Aqf 3 is the main hydraulic unit in the area, in which groundwaters may move along different flowpaths: (i) relatively shallow flowpaths, with no interactions with the Triassic evaporites; and (ii) deeper flowpaths with variable interactions with the Triassic evaporites. Groundwaters with shallow flowpaths emerge at relatively high elevations along the flanks of the main reliefs, while those with deeper flowpaths tend to converge in the topographic/structural depressions. In the Bosso Valley groundwaters emerge as a sulphate–rich spring with a discharge rate in the range 100–200 l/s (no. 7, S. Nicolo' spring), and a temperature of 16–18°C, while in the Burano Valley the main discharge system consists of pressurised groundwaters (up to 22 atm) intercepted by wells drilled for potable water at depths of 125–260 m (wells 16 and 17). According to Bison et al. (1995), the imperviousness of the first 120 m of the 'Massiccio' limestone in the Burano valley is due to the occurrence of an extensive secondary calcite mineralization, which seems to disappear at depth >120–130 m. Sealing must also be present throughout the eastern flank of the Burano Valley, affecting both the upper horizons of the 'Massiccio' formation (up to 450 m a.s.l.) and the pervious layers of the 'Corniola' formation, and causing confinement of the deep water flows coming from the Mt Acuto–Mt Catria area. The scanty information available (drillings and the SW occurrence of natural emergences ('Fontacce' springs)) suggest that the calcite-sealed zone may have a lenticular shape. Bison et al. (1995) suggested the existence of a unique, common recharge system for basal Aqf 3 originating from both the Mt Nerone and the Mt Catria areas. This system emerges naturally along the Bosso Valley (S. Nicolo' Spring) while it is intercepted by wells along the Burano Valley. At present the evaluation of the recharge/discharge balance of this water reservoir is based on the model by Bison et al. (1995).

3. Chemistry of spring and well waters

The physico-chemical characteristics and the results of the monthly chemical monitoring of

Table 1
Physical characteristics and pH of water samples

No.	Sample	Temperature (°C)			pH			Conductivity (mS/cm)			Discharge rate (l/s)		
		Mean	Min	Max	Mean	Min	Max	Mean	Min	Max	Mean	Min	Max
Group A													
1	Palirosa	10.9	9.5	11.7	7.6	7.5	7.7	274	260	290	1.4	1.0	2.0
6	Presa Ca' Baldella	10.1	9.0	10.9	7.9	7.7	8.0	240	230	250	7.9	1.5	15.0
10	Grottone	10.3	9.0	11.8	7.8	7.6	8.0	296	290	300	6.0	1.2	8.0
11	Pelea	11.2	10.5	12.2	7.2	6.9	7.4	302	300	305	1.3	0.8	1.5
12	F.te Luca	9.7	9.0	10.0	7.7	7.6	7.8	258	250	265	2.2	1.3	4.0
Group B													
2	F.te del Sambuco	10.5	10.5	11.5	7.6	7.5	7.7	253	253	260	2.4	0.2	3.2
4	G.tta del Borghetto	–	–	–	7.6	7.5	7.7	230	220	240	–	–	–
5	F.ti del Giordano	10.0	10.0	10.2	7.9	7.3	8.1	245	240	250	71.2	55.2	76.1
13	F.te del Faggio	6.9	6.8	7.0	7.6	7.5	7.7	187	180	190	0.8	0.6	0.9
14	F.te Cupaie	4.9	4.8	4.9	7.6	7.5	7.7	178	170	190	1.2	1.0	1.3
15	PIEIA 2	10.7	10.7	10.7	7.5	7.4	7.5	267	260	270	–	–	–
Group C													
3	F.te del Vitoschio	13.9	12.2	16.4	7.5	7.4	7.5	504	420	590	–	–	–
7	S. Nicolo'	16.5	16.4	16.6	7.9	7.8	8.0	1035	995	1060	127.5	95.0	160.0
Group D													
16	Cagli Acquedotto	11.8	11.5	12.1	7.5	7.4	7.5	488	470	510	–	–	–
17	Cagli 1	11.3	11.3	11.3	7.5	7.4	7.5	424	420	430	–	–	–
B1	Burano 1	12.4	12.0	12.8	–	–	–	402	400	405	–	–	–
Group E													
8	Fontacce 2	10.9	10.8	10.9	7.6	7.5	7.7	359	330	370	–	–	–
9	Fontacce 1	10.9	10.7	11.0	7.6	7.5	7.7	343	320	360	1.8	1.4	2.0

eighteen springs and wells belonging to Aqf 2 and Aqf 3 carried out from January to June 1998 are shown in Tables 1 and 2. Five representative emergences in the area were collected for Aqf 2, and 13 for Aqf 3. Samples were collected and analysed for major ions using standard analytical methods described by Bencini et al. (1977). Samples are grouped as follows: (A) springs from unconfined aquifers emerging from the 'Maiolica' formation (Aqf 2) at altitudes in the range 450–900 m a.s.l., characterized by relatively low discharge rates (<15 l/s) (Table 1); (B) springs and wells from unconfined aquifers emerging from the 'Massiccio' formation (Aqf 3) at relatively high elevation (500–600 m a.s.l.), with large seasonal variability of discharge rate and negligible sulphate contents; (C) linear springs (Boni et al., 1986) from confined aquifers emerging from the 'Massiccio' formation at the lowest elevations (<400 m a.s.l.), characterized by high discharge rate (100–200 l/s) and sulphate concentrations (600–700 mg/l); (D) wells from the confined aquifer of the 'Massiccio' formation located in the topographycally low Burano Valley (<400 m a.s.l.); and (E) springs from unconfined aquifers emerging from the topographically low Burano Valley, characterized by low discharge rates (<2 l/s) and moderately high sulphate concentrations (60–100 mg/l).

Salinity (expressed as TDS: Total Dissolved Solutes) ranges from a minimum value of 174 mg/l measured in May 1998 at Cupaie Spring (group B) to a maximum of 1198 mg/l measured in the same period at S. Nicolo' Spring (group C). Calcium and magnesium are the most representative cations, varying from 39 at Faggio Spring (group B) to 210 mg/l at S. Nicolo' Spring and from 1 at Faggio Spring to 76 mg/l at S. Nicolo' Spring respectively. Accordingly, Ca/Mg ratios also display a large variation among the investigated samples from 3 at S. Nicolo' Spring to 45 at Faggio Spring. On the contrary, sodium and potassium have lower and more homogeneous concentrations both in time and space in the range 3.1–7.0 and 0.1–1.0 mg/l, respectively. Sulphate concentrations displays the largest fluctuation among anions, with concentrations ranging from

Table 2
Chemical composition (mg/l) of water samples

No.	TDS			Na^+			K^+			Ca^{2+}			Mg^{2+}			SO_4^{2-}			Cl^-			HCO_3^-		
	Mean	Min	Max	Mean	Min	Max	Mean	Min	Max	Mean	Min	Max	Mean	Min	Max	Mean	Min	Max	Mean	Min	Max	Mean	Min	Max
Group A																								
1	277	233	297	6	5	6	0.5	0.4	0.5	54	52	55	10	8	12	19	15	23	15	14	18	182	170	193
6	257	244	265	5	5	6	0.3	0.2	0.4	54	52	55	5	3	8	6	2	8	11	9	14	175	165	183
10	318	305	318	5	4	5	0.3	0.5	0.4	63	61	64	10	7	12	5	2	6	13	11	14	223	214	250
11	327	312	327	5	4	5	0.4	0.3	0.5	68	67	70	6	6	8	5	3	6	11	7	13	232	217	256
12	275	268	275	6	5	6	0.9	0.9	0.9	56	55	58	6	4	8	5	2	7	13	11	14	188	181	201
Group B																								
2	276	268	287	5	5	5	0.2	0.2	0.3	57	55	58	7	4	11	3	2	6	12	11	14	191	177	205
4	238	233	243	6	4	7	1.4	0.3	2.7	49	49	49	5	5	7	3	2	5	12	10	14	162	153	168
5	271	253	303	5	4	5	0.5	0.5	0.6	52	52	55	8	5	10	4	1	7	10	10	11	191	175	226
13	193	185	203	4	4	4	0.5	0.5	0.5	40	40	43	4	1	5	6	4	7	10	10	11	129	122	140
14	183	174	191	3	3	3	0.5	0.5	1.1	39	37	43	3	1	5	2	0	4	8	7	10	127	122	135
15	283	272	300	6	5	6	0.9	0.9	1.1	55	52	58	8	6	10	6	3	7	12	11	14	196	181	211
Group C																								
3	521	475	595	7	6	9	0.6	0.5	0.9	102	85	119	19	11	25	174	113	236	15	13	16	204	193	241
7	1156	1113	1198	6	6	7	0.9	0.8	1.0	204	195	210	71	66	76	690	647	731	14	14	15	170	160	177
Group D																								
16	490	472	511	4	4	5	0.7	0.7	0.8	91	88	97	25	24	30	192	184	213	13	11	14	163	153	170
17	431	424	438	4	4	4	0.7	0.7	0.7	76	76	76	23	22	24	154	144	167	12	11	13	161	153	171
B1	414	401	436	4	4	5	0.7	0.7	0.8	71	70	73	22	19	23	139	127	150	11	10	12	165	150	181
Group E																								
8	364	348	382	6	6	7	0.6	0.6	0.8	67	67	70	17	13	20	88	44	111	12	11	13	173	153	206
9	350	329	368	5	4	9	0.6	0.5	0.7	65	60	67	15	12	18	79	54	103	12	11	13	174	162	182

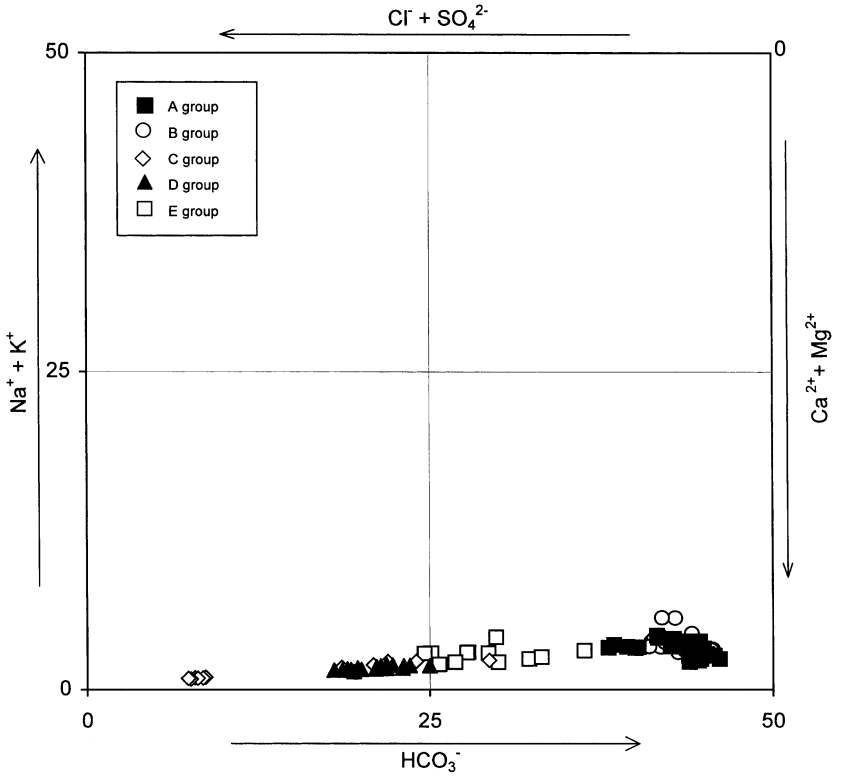

Fig. 3. Square classification diagram (Langelier and Ludwig, 1942) of the water samples. Closed squares, group A; open circles, group B; diamonds, group C; closed triangles, group D; open squares, group E. See text for complete discussion.

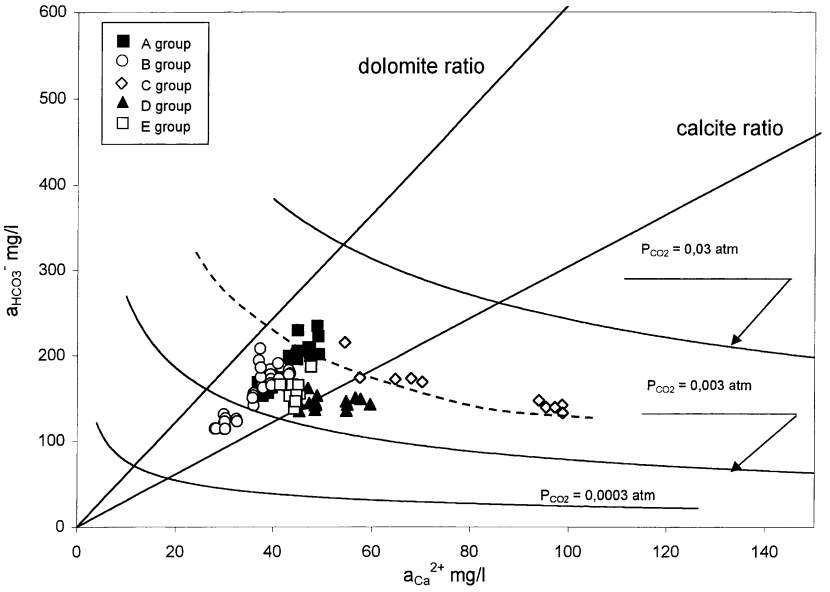

Fig. 4. Ca^{2+} versus HCO_3^- activities of the water samples. Calcite saturation curves are reported for different P_{CO_2}, together with the expected concentration ratios due to calcite and dolomite dissolution according to the following reactions: $CaCO_3 + H_2O + CO_2 = Ca^{2+} + 2HCO_3^-$; $CaMg(CO_3)_2 + H_2O + 2CO_2 = Ca^{2+} + Mg^{2+} + 4HCO_3^-$. Symbols as in Fig. 3.

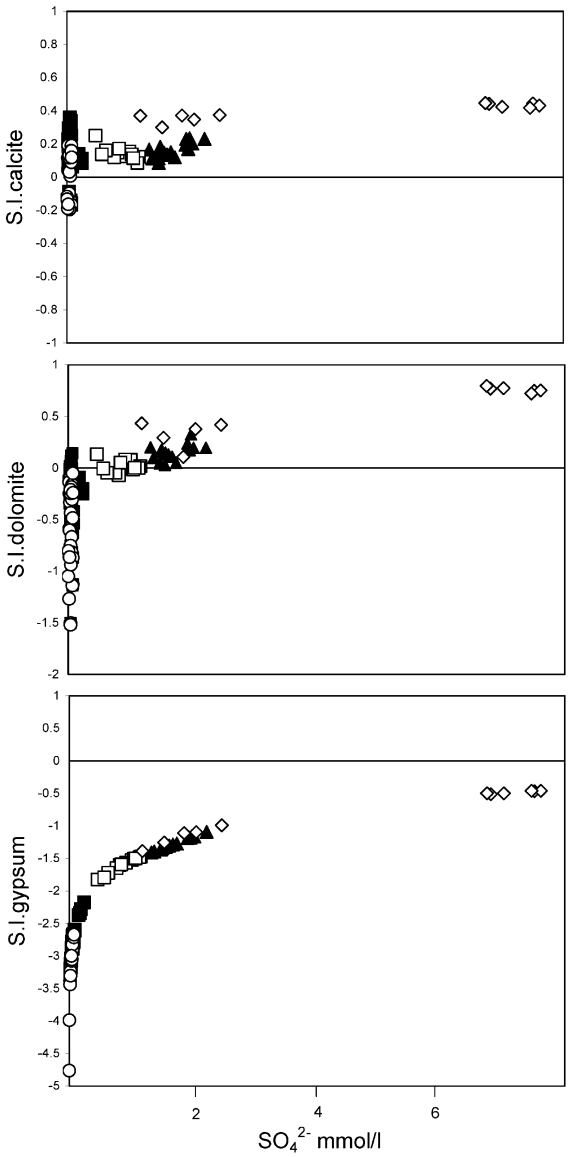

Fig. 5. Saturation indexes (S.I.; Langmuir, 1971) for dolomite, calcite and gypsum plotted versus SO_4^{2-} concentrations of the analysed water samples. Symbols as in Fig. 3.

0.1 at Cupaie Spring to 730 mg/l at S. Nicolo' Spring, while bicarbonate and chlorine ions appear more uniformly distributed, in the range of 120–250 mg/l and 7–16 mg/l, respectively.

According to the Langelier and Ludwig (1942) classification diagram (Fig. 3), the water samples show a linear trend from the Ca-HCO_3 composition of waters of groups A and B to the $CaSO_4$ composition of waters in group C. With the exception of waters pertaining to group B, waters emerging from the limestones of the 'Massiccio' formation are of Ca(Mg)–HCO_3–SO_4, Ca(Mg)–SO_4–HCO_3 and $CaSO_4$ types (groups C, D and E), with an almost continuous series between them. The linear arrangement of the compositions, clearly pointing to the $CaSO_4$ corner, together with the observed progressive increase of dissolved salts, suggest a derivation of the sulphate water types from a progressive dissolution of anhydride or gypsum, or mixing between $CaSO_4$ waters and an original Ca-HCO_3 water.

Fig. 4 shows Ca^{2+} versus HCO_3^- ion activities for the analysed waters together with calcite saturation curves calculated at different P_{CO_2} and the expected Ca^{2+}/HCO_3^- ratios for dolomite and calcite dissolution. Several samples appear saturated with respect to calcite in the P_{CO_2} range 0.003–0.03 atm. Moreover, most of them appear to be arranged along a straight line between dolomite and calcite ratios (groups A, B and E), while samples from the S. Nicolo' Spring and Vitoschio River (group C) and, to a lesser extent, samples from wells in the Burano Valley (group D) tend to be aligned along saturation curves towards the side of Ca^{2+} excess.

Fig. 5 shows a comparison of calcite, dolomite and gypsum saturation indexes of water samples (S.I. = log IAP/Kps, according to Langmuir, 1971) as a function of total dissolved sulphate concentration. Groundwaters are saturated with respect to calcite, regardless of the sulphate concentration and lithology of the rock aquifer. Larger differences and a better defined relationship with sulphate concentration are displayed by the saturation index of dolomite. Groundwaters with low sulphate contents (up to 1 mmol/l) appear to range between dolomite undersaturation to saturation. Conversely, samples with the highest sulphate concentrations, such as those from the Vitoschio River, S. Nicolo' Spring and, to a lesser extent, Burano wells, are oversaturated with respect to dolomite. Saturation degrees for gypsum range from strongly undersaturated to quasi-saturated (S. Nicolo' spring, S.I. = − 0,4). The saturation degrees of S. Nicolo' Spring may imply a quasi-equilibrium between water and gypsum or a mixing process between a gypsum or anhydrite-saturated water and a Ca-HCO_3 water with a mixing ratio of about 2:1.

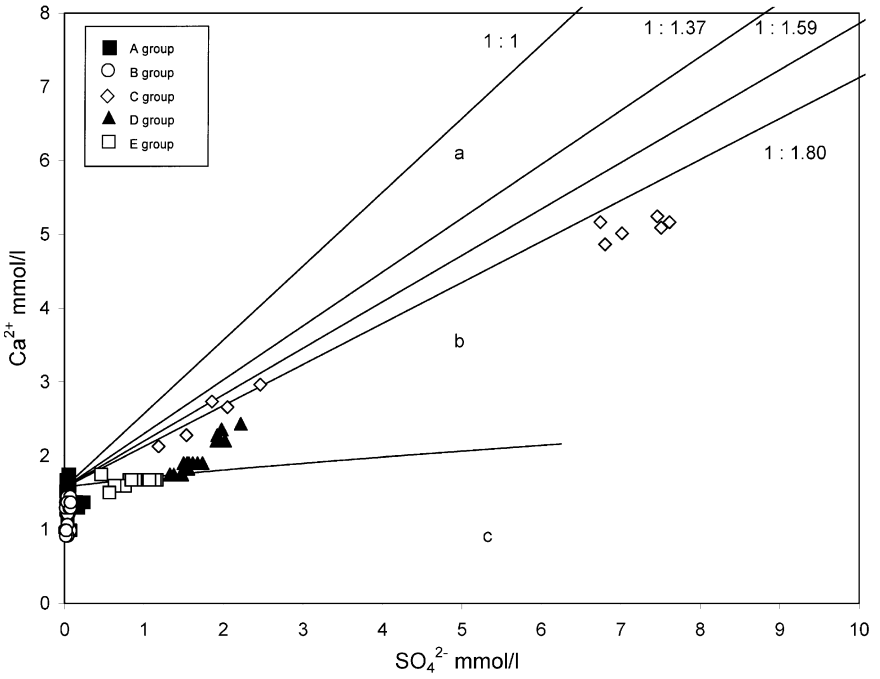

Fig. 6. Ca^{2+} versus SO_4^{2-} concentrations of the analyzed water samples. Starting from calcite-saturated waters at $P_{CO_2} = 0.003$, solid lines represent the expected evolutions of Ca^{2+}/SO_4^{2-} ratios due to gypsum dissolution, dedolomitization and calcite precipitation. (a): Gypsum dissolution without calcite precipitation. (b): Gypsum dissolution, dedolomitization and calcite precipitation in a 'closed system' for CO_2. The different ratios result from different degrees of dolomite and calcite oversaturation (after Appelo and Postma, 1993, modified). (c) Gypsum dissolution and calcite precipitation in an 'open system' for CO_2. Symbols as in Fig. 3.

Since anhydrite occurs in the Triassic evaporites (Martinis and Pieri, 1964), its actual conversion into gypsum may explain the higher temperature (16°C) measured at S. Nicolò Spring in comparison with the regional mean temperature (10°C). Anhydrite releases 27.32 kcal/mole when it is converted to gypsum. Therefore, the temperature excess of the S. Nicolo' Spring may be caused by the conversion of 25 g/l of anhydrite to gypsum or, if we consider the mixing ratio defined above and the $CaSO_4$-saturated end member, 48 g/l of anhydrite.

The possible effects of dissolution of gypsum on Ca^{2+} versus SO_4^{2-} concentrations are shown in Fig. 6. Three different trends of chemical evolution are considered (after Appelo and Postma, 1993, modified): (a) gypsum dissolution without calcite precipitation; (b) calcite precipitation and dedolomitization in 'closed system' conditions, at three different supersaturation states for dolomite and calcite (Back and Hanshaw, 1970; Atkinson, 1983; Back et al., 1984; Plummer et al., 1990); and (c) gypsum dissolution and calcite precipitation at constant P_{CO_2} ('open system' conditions). Condition (a) results from gypsum dissolution in calcite-undersaturated conditions or from kinetically-controlled dissolution–precipitation processes. Condition (c) represents gypsum dissolution at constant P_{CO_2}, i.e. the occurrence of an infinite source of CO_2, which induces continuous calcite precipitation. In this case, Ca^{2+} concentration undergoes only a slight increase due to the increasing ionic strength of the solution (ionic strengths and activity coefficients are calculated at increments of 100 mg/l of SO_4^{2-} starting from pure water in equilibrium with calcite). Condition (b) refers to dedolomitization processes as described by Back et al. (1984); Plummer et al. (1990). The dedolomitization process can be summarized as follows (Plummer et al., 1990):

$$1.8CaSO_4 + 0.8CaMg(CO_3)_2 \rightarrow 1.6CaCO_3 + Ca^{2+} + 0.8Mg^{2+} + 1.8SO_4^{2-}$$

This process leads to an irreversible dolomite →

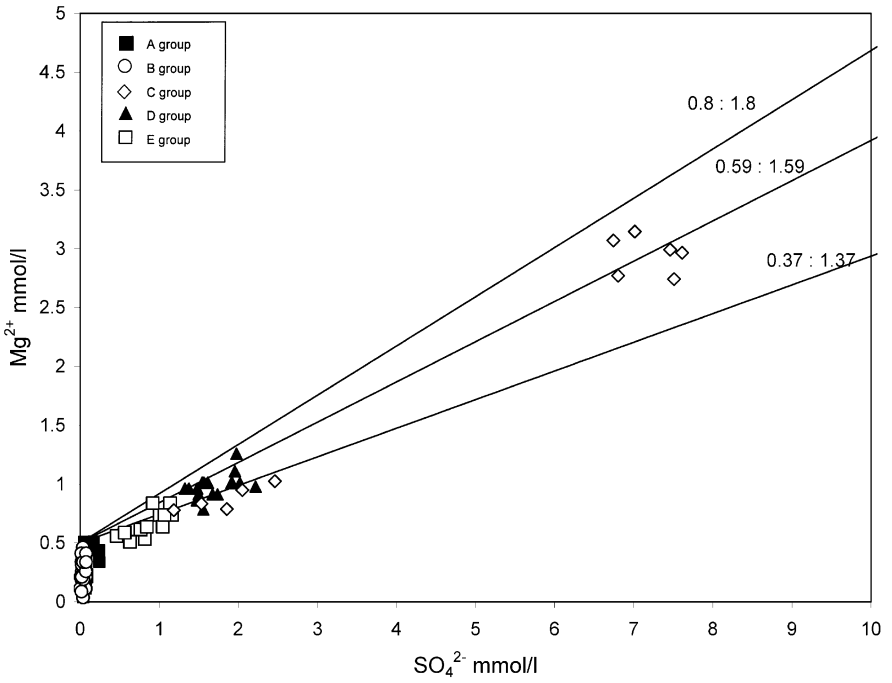

Fig. 7. Mg^{2+} versus SO_4^{2-} concentrations for the water samples. Solid lines represent the expected evolution of the Mg^{2+}/SO_4^{2-} ratios due to dedolomitization and calcite precipitation (after Appelo and Postma, 1993, modified). The different ratios result from different degrees of dolomite and calcite oversaturation. For explanation see text. Symbols as in Fig. 3.

calcite transformation as a result of gypsum dissolution in a closed system for CO_2, where the initial amount of CO_2 is consumed by progressive calcite precipitation. In this case Ca^{2+} and Mg^{2+} concentrations in solution increase due to both gypsum and dolomite dissolution. The three lines represent three different stoichiometries of the mass transfer reaction respectively referring to perfect dolomite/calcite saturation conditions ($Ca/SO_4 = 1{:}1.8$), dolomite equilibrium and calcite supersaturation at $S.I._{cc} = 0.15$ ($Ca/SO_4 = 1{:}1.37$) and, finally, dolomite and calcite supersaturation at $S.I._{dol} = 0.7$ and $S.I._{cc} = 0.4$, respectively, ($Ca/SO_4 = 1{:}1.59$). The corresponding Mg/SO_4 ratios for the dedolomitization process are reported in Fig. 7. Unlike Appelo and Postma (1993), the intercept in the Mg axis has been adapted to 0.5 mmol/l, i.e. the mean concentration value of the sulphate-free, dolomite undersaturated samples, whose Mg contents can be mainly related to dissolution of Mg calcite. A careful inspection of Figs. 6 and 7 reveals that, among others, the Vitoschio River and the S. Nicolo' Spring (group C) more closely match the dedolomitization patterns for both Ca^{2+}/SO_4^{2-} and Mg^{2+}/SO_4^{2-} values. Ca^{2+} versus SO_4^{2-} patterns for Fontacce 1 and 2 springs (group E) deviate from the dedolomitization pattern, better fitting with a mechanism controlled by gypsum-induced calcite precipitation in 'open system' conditions, i.e. at constant P_{CO_2} (0.003 atm). The trend of the Burano wells (group D) seems to be a sequential evolution from the Fontacce type waters, but aligned with the isomolar Ca^{2+}/SO_4^{2-} ratio, implying gypsum dissolution without calcite equilibration.

If we consider the areal distribution of the emergence points in relation to potential recharge areas, we see that an approach to dedolomitization only occurs for waters recharged in the Mt Nerone area, whereas 'open system' calcite precipitation followed by pressurization below the resulting calcite sealed zone occurs in the Burano Valley recharged from the Mt Acuto–Mt Catria area. According to both the observed chemical behaviour and the hydrogeological information,

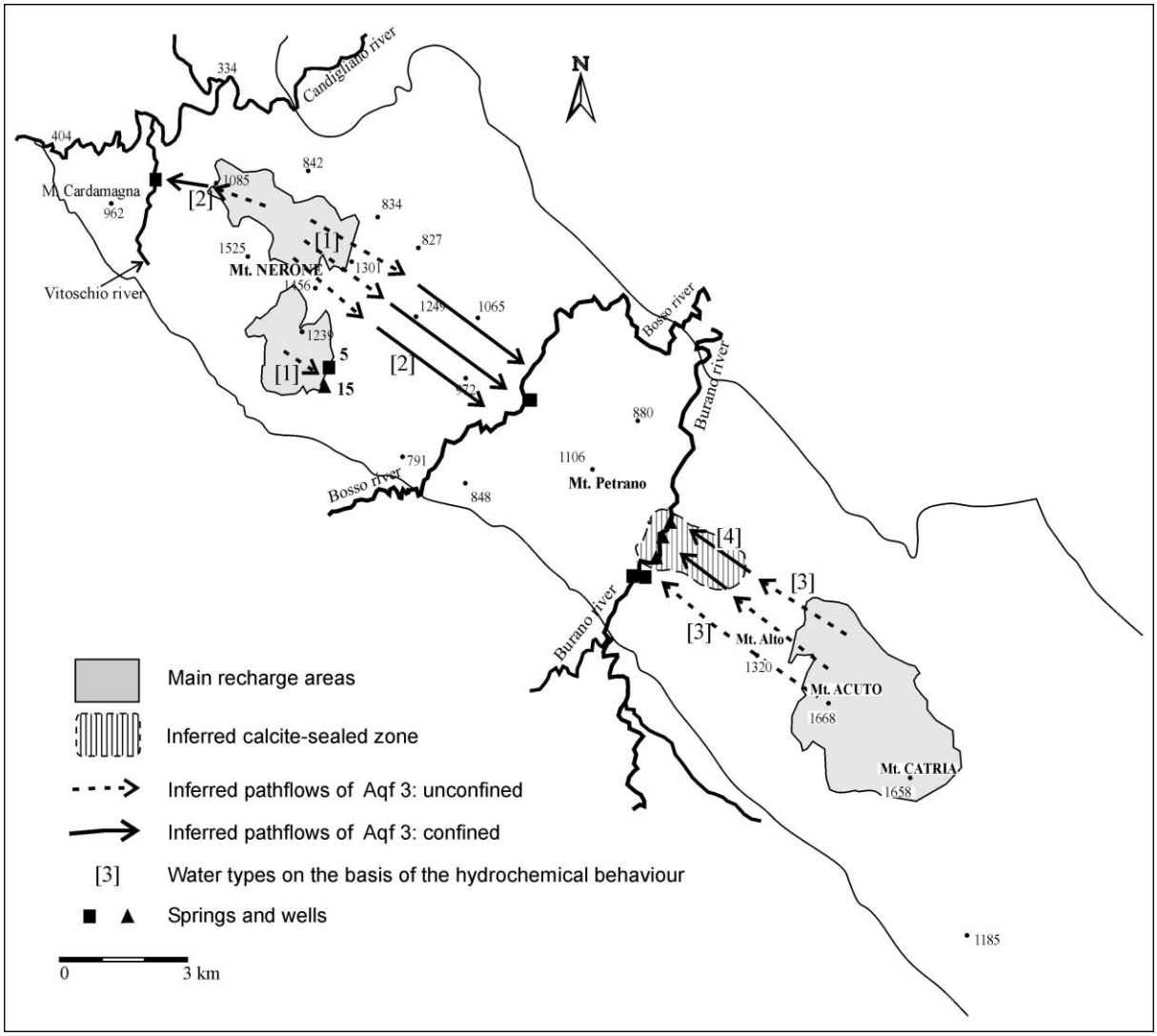

Fig. 8. Inferred flowpaths and water types of Aqf 2 and Aqf 3 in the area under study. Dashed arrows: pathflows in unconfined or 'open system' conditions; solid arrows: pathflows in confined or 'closed system' conditions. The shaded area shows the calcite-sealed zone. The other symbols as in Fig. 1.

the most reasonable pathflows (both confined and unconfined) for groundwaters throughout Aqf 3 are reported in Figs. 8 and 9. Striking differences in the measured discharge rates, also suggest that there are no interconnections between the Mt Nerone and Mt Catria sectors. This implies that the area of Mt Petrano probably acts as an impervious barrier between the two hydraulic systems.

4. Conclusions

The available chemical and hydrological data on spring and well waters of the Mt Catria–Mt Nerone ridge indicate the general occurrence of gypsum dissolution which causes calcite precipitation under different P_{CO_2} conditions between the Bosso and the Burano valleys. Accordingly, we have distinguished four types of hydrochemical behaviour.

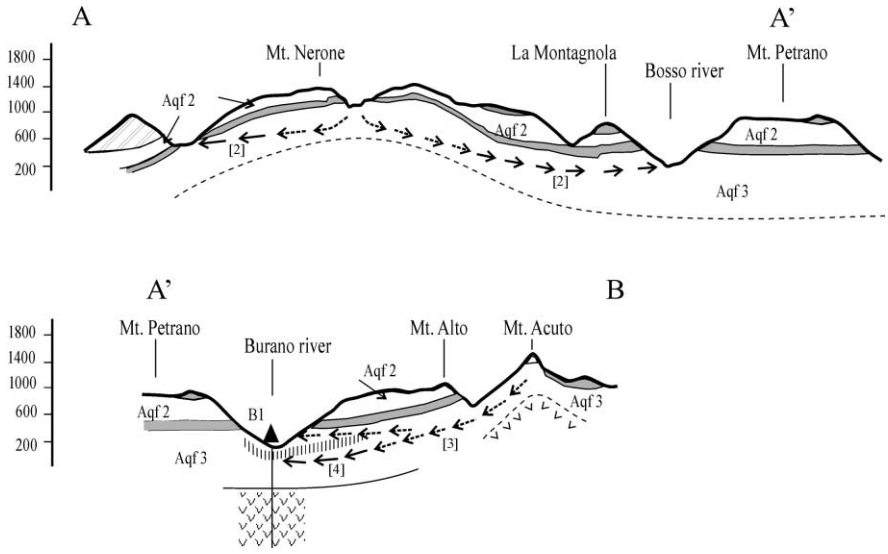

Fig. 9. Schematic NW–SE cross section with inferred flowpaths and water types of the basal Aqf 3 in the area under study. Vertical exaggeration is 1.7:1. Dashed arrows: pathflows in unconfined or 'open system' conditions; solid arrows: pathflows in confined or 'closed system' conditions. The shaded area shows the calcite-sealed zone. The dashed line represent the inferred location of the top of the Evaporites formation. The other symbols as in Fig. 2.

1. *Ca-HCO_3 waters*. This includes waters that do not display any evidence of interaction with gypsiferous layers emerging from both the 'Maiolica' and the 'Massiccio' formations (groups A and B) (Figs. 8 and 9). Usually unsaturated with respect to dolomite and saturated to supersaturated with respect to calcite, they are indistinguishable on the basis of major ions only. As depicted in Fig. 8, their flowpaths are short and, probably, relatively shallow.
2. *Ca-(HCO_3)– SO_4 and $CaSO_4$ waters affected by dedolomitization in a closed CO_2system*. These types are confined to the northwestern sector of the Mt Catria–Mt Nerone ridge, emerging at S. Nicolo' Spring and along the Vitoschio River (group C). As shown in Figs. 8 and 9, and consistent with isotopic data (Bison et al., 1995), their recharge area is located close to Mt Nerone. According to the structural elevation of the area, their deep flowpaths appear to be controlled by the structure of the Triassic evaporites, which act as a hydrogeological watershed at depth. Dissolution–precipitation processes occur in a closed system which implies at least partially confined conditions in the final part of the pathflows (Fig. 8). The presence of a finite source of CO_2 is also confirmed by the large deviation of Ca/HCO_3 ratios from the rock compositions along a saturation curve for the Vitoschio River and S. Nicolo' Spring (Fig. 4).
3. *Ca-(HCO_3)– SO_4 calcite-precipitating waters at constant P_{CO_2} ('open system' behaviour).* This type of water emerges in the Burano Valley (Fontacce samples, group E) and comes from the recharge area of Mt Catria (Figs. 8 and 9). As confirmed by the extensive calcite encrustation observed at their emergence points, the water from these springs precipitates calcite in an 'open system' for CO_2. As also confirmed by the constant Ca^{2+}/HCO_3^- ratios (Fig. 4), this prevents any relative increase of Ca^{2+} contents due to gypsum dissolution and calcite precipitation. We suggest that waters of this type are responsible for the observed general fracture sealing of the 'Massiccio' limestone along the Burano Valley. Fracture sealing is probably still occurring today. Calcite actually precipitates at constant $P_{CO_2} \approx 0.003$ atm, which is a typical P_{CO_2} pressure existing in the water-saturated zone of the soil that can be extended throughout the whole unsaturated zone due to rapid gas exchange through the gas phase (Laursen, 1991). Therefore, sealing occurs close to phreatic, unconfined conditions (Fig. 8).

4. *Ca-(HCO_3)– SO_4 waters from pressurized aquifers.* This type of water (group D) appears to be sequentially evolved from type (E) waters due to further gypsum dissolution without significant calcite precipitation (Figs. 8 and 9). This is probably caused by a transition from 'open' to 'closed system' and pressurization, which also explains the slight deviation of the Ca/HCO_3 ratios from the rock composition.

Accordingly, we believe that group E waters may represent the residue of an ancient unconfined flow, which evolved into the present confined and pressurized flow of group D waters due to calcite precipitation and sealing.

In conclusion, basal Aqf 3 must be subdivided into two almost independent hydraulic units with two independent recharge and discharge areas (Fig. 8): (i) the Mt Catria area which supplies waters for wells and springs (groups D and E) in the Burano Valley, with the highest discharge rates; and (ii) the Mt Nerone area which supplies waters for the Vitoschio Valley and S. Nicolo' Spring (group C). This may also explain the different regimes of observed hydraulic pressures of the basal aquifer between the Bosso and Burano valleys.

References

Alvarez, W., 1989a. Evolution of the Monte Nerone seamount in the Umbria–Marche Apennines. 1. Jurassic–Tertiary stratigraphy. Boll. Soc. Geol. It. 108-1, 3–21.

Alvarez, W., 1989b. Evolution of the Monte Nerone seamount in the Umbria–Marche Apennines. 2. Tectonic control of the seamount–basin transition. Boll. Soc. Geol. It. 108-1, 23–39.

Appelo, C.A.J., Postma, D., 1993. Geochemistry, Groundwater and Pollution. A.A. Balkema, Rotterdam.

Atkinson, T.C., 1983. Growth mechanism of speleothems in Castleguard cave, Columbia icefields, Alberta Canada. Arct. Alpine Res. 15, 523–536.

Back, W., Hanshaw, B.B., 1970. Comparison of chemical hydrogeology of the carbonate peninsula of Florida and Yucatan. J. Hydrol. 10, 330–368.

Back, W., Hanshaw, B.B., Plummer, L.N., Rahn, P.H., Rightmire, C.T., Rubin, M., 1984. Process and rate of dedolomitization: mass transfer and 14C dating in a regional carbonate aquifer. Geol. Soc. Am. Bull. 94, 1415–1429.

Barchi, M.R., De Feyter, A., Magnani, M.B., Minelli, G., Pialli, G., Sotera, B.M., 1998. The structural style of the Umbria–Marche fold and thrust belt. Mem. Soc. Geol. It. 52, 557–578.

Bencini, A., Duchi, V., Martini, M., 1977. Geochemistry of thermal spring of Tuscany (Italy). Chem. Geol. 19, 229–252.

Bison, P., Mariotti, C., Pieroni, M., Piovesana, F., Priante, M., Pugi, S., 1995. Valutazione e protezione delle risorse idriche sotterranee nella dorsale carbonatica M.Catria–M.Nerone (Marche). Groundwater Geoengineering 5, 13–24.

Boni, C., Bono, P., Capelli, G., 1986. Schema idrogeologico dell'Italia Centrale (In Italian). Mem. Soc. Geol. It. 35, 991–1012.

Buiter, S.J.H., Wortel, M.J.R., Govers, R., 1998. The role of subduction in the evolution of the Apennines foreland basin. Tectonophysics 296, 249–268.

Centamore, E., Soc. Idrotecneco, Valletta, M., (1976). Note illustrative della Carta Idrogeologica F° 291 'Pergola'. Serv. Geol. d'Italia, Roma. (In Italian).

Hanshaw, B.B., Back, W., 1979. Major geochemical processes in the evolution of carbonate-aquifer systems. J. Hydrol. 43, 287–312.

Jacobacci, A., Centamore, E., Chiocchini, M., Malferrari, N., Martelli, G. and Micarelli, A., (1974). Note esplicative della Carta Geologica d'Italia (1:50,000). Foglio 290—Cagli. Serv. Geol. d'Italia, Roma.

Langelier, W.F., Ludwig, H.F., 1942. Graphical method for indicating the mineral character of natural waters. J. Am. Waterworks Assoc. 34, 335–352.

Langmuir, D., 1971. The geochemistry of some carbonate ground waters in central Pennsylvania. Geoch. Cosmoch. Acta 35, 1023–1045.

Laursen, S., 1991. On gaseous diffusion of CO_2 in the unsaturated zone. J. Hydrol. 122, 61–69.

Martinis, B., Pieri, M., 1964. Alcune notizie sulla formazione evaporitica del triassico superiore nell'Italia centrale e meridionale. Mem. Soc. Geol. It. 4, 649–678.

Passeri, L., 1975. L'ambiente deposizionale della formazione evaporitica nel quadro della paleogeografia del Norico Tosco–Umbro–Marchigiano. Boll. Soc. Geol. It. 94, 231–268.

Plummer, L.N., Busby, J.F., Lee, R.W., Hanshaw, B.B., 1990. Geochemical modeling of the Madison Aquifer in parts of Montana, Wyoming and South Dakota. Water Resour. Res. 26 (9), 1981–2014.

Tavarnelli, E., 1997. Structural evolution of a foreland fold-and-thrust belt: the Umbria–Marche Apennines, Italy. J. Struct. Geol. 19, 523–534.